

CATION DETERMINATIVE CURVES FOR Mg-Fe-Mn OLIVINES FROM VIBRATIONAL SPECTRA¹

ROGER G. BURNS AND FRANK E. HUGGINS, *Department of Earth and
Planetary Sciences, Massachusetts Institute of Technology,
Cambridge, Massachusetts 02139*

ABSTRACT

Infrared spectra in the region 4000-200 cm^{-1} have been measured for several analysed olivine minerals. Ten or more bands are observed below 1000 cm^{-1} , the frequencies of which are composition dependent and move to lower energies with increasing Fe and Mn in the olivine. Best-fit equations relating peak maxima to olivine composition were computed for each of the three binary series and a triangular determinative grid constructed for Mg-Fe-Mn olivines. Deviations from linearity in certain determinative curves of Mg-Mn and Fe-Mn olivines correlate with Mn^{2+} ordering in $M(2)$ positions. The accuracy of an olivine composition determinative curve is inversely proportional to the frequency shift between end-member compositions. In the forsterite-fayalite series, the compositions estimated from bands 4 and 5 in the infrared spectra are as close to the true compositions as estimates based on established X-ray d spacings and cell parameter data.

INTRODUCTION

Numerous schemes have been suggested for estimating semiquantitatively the cation compositions of natural and synthetic olivines (Deer, Howie, and Zussman, 1963, v. 1, p. 3, 7, 20-24). In the forsterite-fayalite series these methods include those based on optical properties (Bowen and Schairer, 1935; Poldervaart, 1950), density (Bloss, 1952), X-ray data (Yoder and Sahama, 1957; Eliseev, 1957; Heckrodt, 1958; Jackson, 1960; Hotz and Jackson, 1963; Jambor and Smith, 1964; Agterburg, 1964; Nafziger and Muan, 1967; Louisnathan and Smith, 1968; Matsui and Syono, 1968; Fisher and Medaris, 1969; Jahanbagloo, 1969), heats of solution (Sahama and Torgeson, 1949), and electronic absorption spectral measurements (Burns, 1970). In the forsterite-tephroite series refractive index and X-ray data have been used to obtain approximate compositions (Hurlbut, 1961; Glasser and Osborn, 1960). Apart from some optical data for knebelite-fayalite compositions (Henriques, 1968) no determinative method has been suggested for the fayalite-tephroite series. Most of the determinative curves for olivines are restricted to two-cation systems only.

¹Paper presented at the 1970 Annual Meetings of the Geological Society of America, Milwaukee, Abstr., p. 511-512.

Early studies of the infrared spectra of olivines (Lehmann, Dutz, and Koltermann, 1961; Duke and Stephens, 1964) have shown that peak maxima are composition dependent. Duke and Stephens (1964) suggested from measurements down to 400 cm^{-1} that infrared spectra could be used as determinative curves for olivines. We have extended the spectral range to 200 cm^{-1} and have derived equations of cation composition determinative curves for the Mg-Fe, Fe-Mn, and Mg-Mn olivine binary solid-solution series, and have constructed a determinative grid for ternary Mg-Fe-Mn olivines.

EXPERIMENTAL METHODS

The chemical analyses of the minerals used in the present study are summarized in Table 1. Specimens 1-11 belong to the forsterite-fayalite series, and specimens 11-15 conform closely to the fayalite-tephroite series, while the tephroite-forsterite series is represented only by specimens 15, 16, 17, and 1. Data are also included for roeperite (specimen 18), monticellite (specimen 19), and willemite (specimen 20). The compositions of the olivines (specimens 1-18) are plotted on a triangular diagram for the Mg_2SiO_4 , Fe_2SiO_4 , and Mn_2SiO_4 components in Figure 1. This figure demonstrates the restricted pseudobinary nature of olivine minerals.

Most of the spectra were measured over the range $2000\text{--}200\text{ cm}^{-1}$ on a Perkin-Elmer model 225 recording spectrophotometer using powdered olivine specimens in pressed cesium iodide discs. The precision of this instrument is such that certain peak maxima may be read to $\pm 0.5\text{ cm}^{-1}$ unit. Sample preparation of silicate minerals for infrared measurements is described elsewhere (Burns and Prentice, 1968; Bancroft and Burns, 1969).

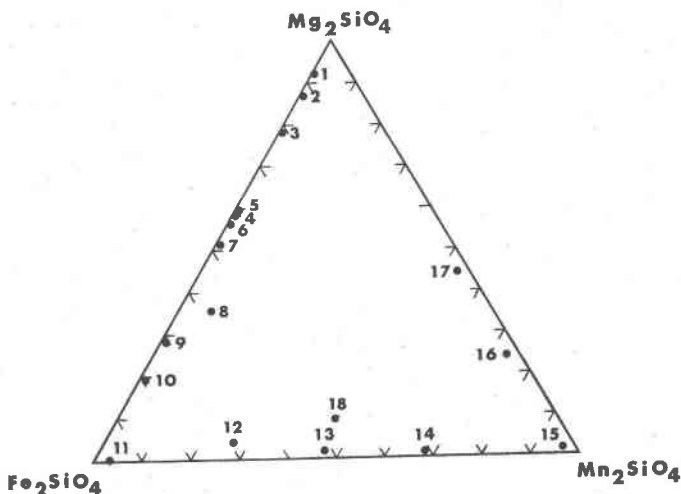


FIG. 1. Compositions of the olivines used for infrared measurements.

Relationships between olivine composition (X) and frequency (ν) of each peak maximum in the infrared spectrum (in cm^{-1} units) were computed by a least squares method, using the CURFIT 2 ALGOL program on file at the Oxford University Computing Laboratory, England. This program enables a series of polynomials up to degree n to be computed, provided there are $(n + 2)$ or more points, together with two statistical error estimates: (1) sum of squares of residuals $\Sigma(|\nu_{\text{obs}} - \nu_{\text{calc}}|^2)$ for all points of coordinates (X, ν) for each polynomial having the form

$$\nu = c(n, 0) + c(n, 1)X + \cdots + c(n, n) X^n$$

and (2) standard deviations $d(n, q)$ for the corresponding coefficients $c(n, q)$. The best-fit polynomial relating peak maxima to olivine composition was taken to be that for which the ratio residual (n): residual ($n + 1$) did not exceed 2:1.

RESULTS

The spectra of minerals with the olivine structure are remarkably similar in the region $1000\text{--}550 \text{ cm}^{-1}$. This is illustrated by Figure 2, in which the spectra of the olivines forsterite, fayalite, tephroite, and monticellite are compared with that of willemite which does not have the olivine structure. Five peaks may be distinguished in this region, the positions of which change with cation content of the olivine. An additional seven or eight peaks may be recognized in the region below 550 cm^{-1} , the relative intensities and positions of which may vary with olivine composition.

The spectra of the forsterite-fayalite series (except specimen 8, which contains appreciable Mn) are illustrated in Figure 3 and the positions of the peak maxima are summarized in Table 2. Thirteen peaks or prominent shoulders could be identified in the spectrum of forsterite (specimen 1). Most of the peaks could be traced across the forsterite-fayalite series. Such sets of peaks are here labelled bands 1 to 13.

All of the bands on the forsterite-fayalite series show a shift of peak maxima to lower frequencies with increasing iron content. However, the compositional variations of the individual bands differ, with the result that there are also notable changes of relative intensity and breadth of the band envelopes across the series caused by the merging and divergence of neighboring bands. For example, bands 6 and 7 appear to diverge with increasing iron content, so that band 6, which starts as a prominent shoulder in the spectrum of specimen 1 becomes a distinct peak in the spectra of specimens 5 to 11.

The spectra of the fayalite-tephroite series are illustrated in Figure 4. The same series of bands found for the forsterite-fayalite series are remarkably uniform across the fayalite-tephroite series. The peak maxima data summarized in Table 3 show that the compositional

Table 1. Compositions and Sources of the Olivines^c

Specimen Number	1	2	3	4	5	6	7	8	9	10	11	12	13	14	15	16	17	18 ^a	19 ^b
SiO ₂	41.40	40.71	39.66	36.26	36.80	35.4	35.35	32.66	32.63	31.65	29.70	30.0	28.42	29.6	29.31	n.d.	n.d.	29.35	37.46
TiO ₂	0.00	0.00	0.01	0.02	0.03	0	0.00	0.01	0.05	0.07	0.00	n.d.	0.06	n.d.	n.d.	n.d.	n.d.	n.d.	n.d.
Al ₂ O ₃	0.09	0.06	0.06	0.06	0.06	n.d.	0.02	0.06	0.09	0.04	0.00	n.d.	0.27	n.d.	n.d.	n.d.	n.d.	n.d.	n.d.
Fe ₂ O ₃	0.47	n.d.	n.d.	n.d.	n.d.	n.d.	n.d.	n.d.	n.d.	n.d.	n.d.	n.d.	n.d.	n.d.	n.d.	n.d.	n.d.	n.d.	n.d.
FeO	7.92	10.89	19.60	34.37	34.38	38.3	41.15	48.58	55.50	59.15	68.60	49.5	36.21	22.15	1.67	1.90	1.40	30.3	3.98
MnO	0.13	0.16	0.27	0.48	0.47	0.5	0.54	4.78	0.39	0.94	2.00	18.6	32.26	47.0	65.62	46.19	32.82	29.4	0.52
MgO	49.25	47.14	40.95	28.05	28.80	25.2	23.50	13.66	11.90	8.39	0.10	1.85	0.90	0.5	0.71	8.72	15.76	3.45	22.78
CaO	0.07	0.60	0.07	0.10	0.08	0.1	0.03	0.06	0.11	0.19	0.01	0.1	0.07	0.5	0.70	tr	0.10	0.25	35.20
NiO	0.34	0.18	0.27	0.10	0.10	0	0.15	0.02	0.00	0.00	0.00	n.d.	n.d.	n.d.	n.d.	n.d.	n.d.	n.d.	n.d.
Others	0.04	--	--	--	--	--	--	--	--	--	--	--	0.03	--	--	--	--	7.10	0.15
Total	99.71	99.74	100.89	99.44	100.72	99.5	100.74	99.83	100.67	100.43	100.41	100.05	98.22	99.85	98.01	--	--	99.75	100.09
Fe ₂ SiO ₄	8.63	11.34	21.02	40.33	39.76	42.85	49.09	62.39	71.78	78.53	96.86	69.0	51.4	31.1	1.0	2.70	2.50	41.5	
Mg ₂ SiO ₄	90.81	87.51	78.30	58.82	59.46	56.55	50.04	31.27	27.51	19.85	0.24	4.6	2.2	1.3	4.2	24.10	44.50	8.4	
Mn ₂ SiO ₄	0.14	0.17	0.30	0.58	0.54	0.50	0.65	6.22	0.51	1.28	2.88	26.2	46.4	66.8	93.7	73.20	52.80	41.0	
Ca ₂ SiO ₄	0.10	0.80	0.10	0.16	0.11	0.10	0.04	0.10	0.19	0.34	0.02	0.2	--	0.9	1.2	--	--	0.4	
Ni ₂ SiO ₄	0.33	0.18	0.28	0.11	0.13	0	0.18	0.02	0	0	--	--	--	--	--	--	--	--	

a) includes 7.10% ZnO or 8.6 mole% Zn₂SiO₄

b) formula Cal.003Mg0.904Fe0.089Mn0.012Si0.897O4

c) specimen 2c, willowite, not analysed.

TABLE 1, CONT.

1. Forsterite; Webster, North Carolina; analysts: J. Carpenter, D. G. W. Smith (microprobe).
2. Chrysolite; Jan Mayan Island, Arctic Ocean (Berkeley 12489); analyst: D. G. W. Smith (microprobe).
3. Chrysolite; Skaergaard intrusion, East Greenland (Oxford 4526); analyst: D. G. W. Smith (microprobe).
4. Hyalosiderite; Skaergaard intrusion, East Greenland (Oxford 5107); analyst: D. G. W. Smith (microprobe).
5. Hyalosiderite; Skaergaard intrusion, East Greenland (Oxford 5111); analyst: D. G. W. Smith (microprobe).
6. Hyalosiderite; Skaergaard intrusion, East Greenland (Oxford 4077); analyst: J. V. Smith (1966).
7. Hyalosiderite; Lydenburg, Transvaal, South Africa (Cambridge 54087); analyst: D. G. W. Smith (microprobe).
8. Hortonolite; location unknown (Berkeley 12494); analyst: D. G. W. Smith (microprobe).
9. Ferrohortonolite; Skaergaard intrusion, East Greenland (Oxford 5181); analyst: D. G. W. Smith (microprobe).
10. Ferrohortonolite; Skaergaard intrusion, East Greenland (Oxford 4147); analyst: D. G. W. Smith (microprobe).
11. Fayalite; Rockport, Massachusetts (USNM R3517); analyst: D. G. W. Smith (microprobe).
12. Knebelite; Schysshytan, Sweden (Berkeley 12511); analyst: D. C. Harris (microprobe).
13. Knebelite; Dannemora, Sweden; analyst: G. E. Brown, personal communication (microprobe).
14. Manganknebelite; Broken Hill, Australia; analyst: D. C. Harris (microprobe).
15. Tephroite; Clark's Peninsula, Wilkes Land, Antarctica; Mason (1959).
16. Picrotephroite; Sterling, New Jersey, U.S.A. (Harvard 105490); analyst: Hurlbut (1961).
17. Picrotephroite; Franklin, New Jersey, U.S.A. (Harvard 85551); analyst: Hurlbut (1961).
18. Roepperite; Franklin, New Jersey, U.S.A. (Harvard Bauer Collection); analyst: D. C. Harris (microprobe).
19. Monticellite; Crestmore, California, U.S.A. (BM 1960, 334); analyst: Moehlman and Gonyer (1934).
20. Willemite; Belgium (Oxford Museum); unanalysed.

variations of all bands for the fayalite-tephroite series are smaller than those for the forsterite-fayalite series (Table 2).

In the forsterite-tephroite series the poor representation of specimens having compositions between 10 and 50 percent Mn_2SiO_4 makes it difficult to correlate bands unambiguously across the series at low frequencies. This region of the infrared spectra is illustrated in Figure 5 and the peak maxima data are summarized in Table 3. The spec-

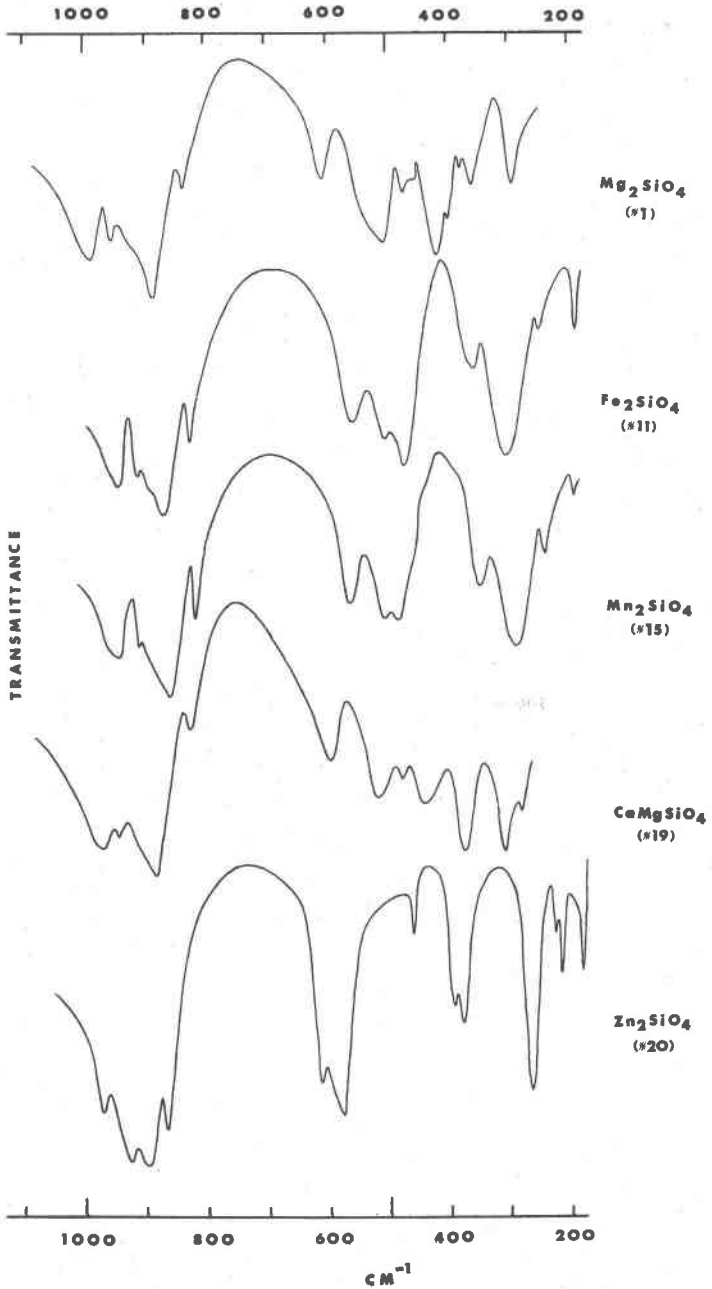


FIG. 2. Comparative infrared spectra of willemite and the olivines forsterite, fayalite, tephroite, and monticellite.

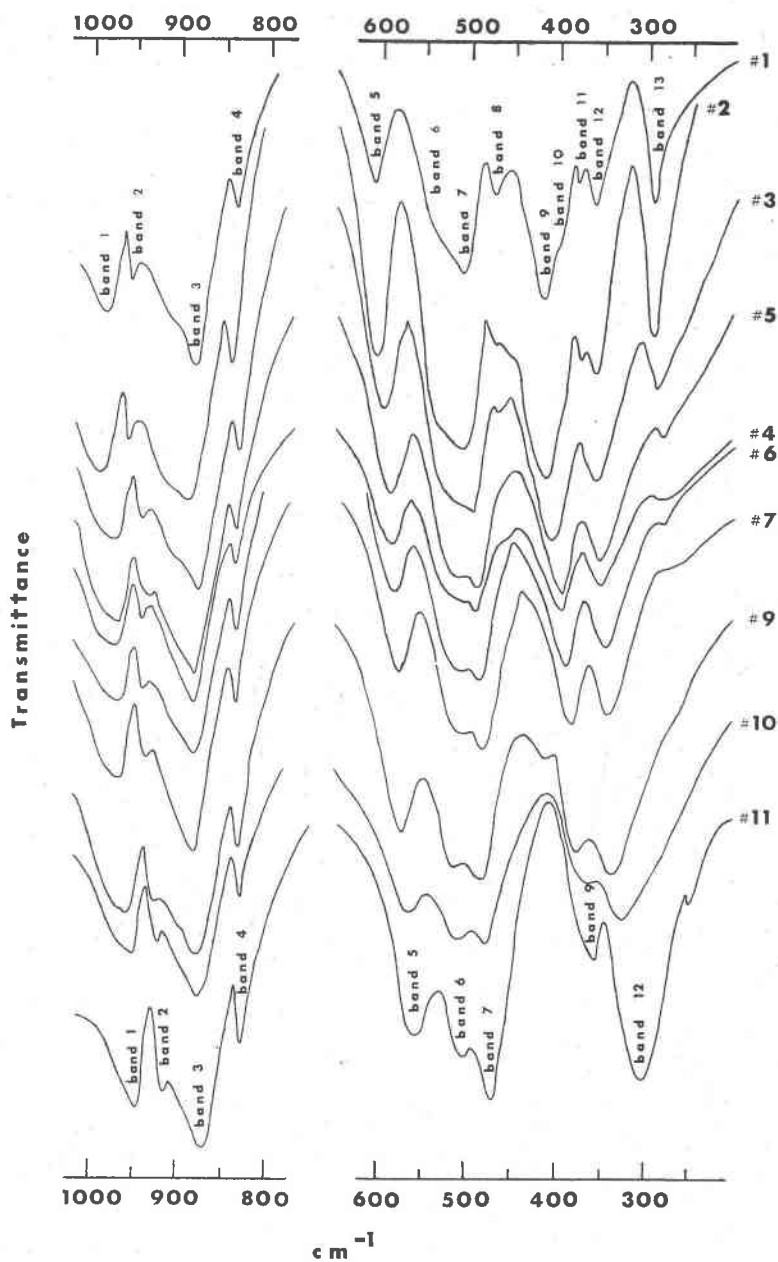


FIG. 3. Infrared spectra of Mg-Fe olivines of the forsterite-fayalite series.

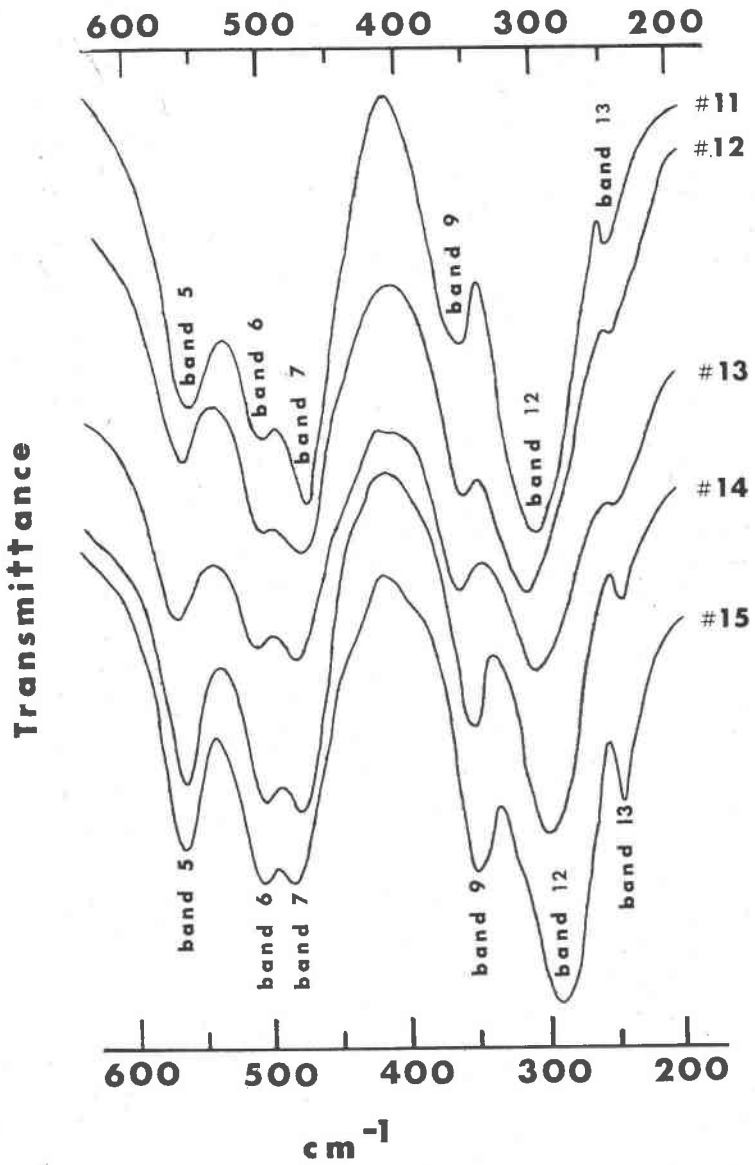


Fig. 4. Infrared spectra of Fe-Mn olivines of the fayalite-tephroite series.

Table 2. Peak maxima in the infrared spectra of olivines
of the forsterite - fayalite series

Specimen No.	1	2	3	4	5	6	7	8	9	10	11
Band 1	982	984	980	967	973	968	965	961	958	950	945
2	954	951	945	935	940	939	935	927	926	919	914
3	885	885	885	882	882	880	881	874	877	876	872
4	838	838	836	834	835	834	833	830	830	829	827
5	605	604	597	588	588	585	583	573	571	568	558
6	s	s	s	s	s	510	513	508	510	510	506
7	506	504	496	490	491	492	487	482	482	480	472
8	469	s	465	s	s	s	s	s	408	s	s
9	415	413	406	394	396	392	390	377	377	366	356
10	399 _s	s	s								
11	378	375	s	s	s						
12	357	358	356	352	350	348	349	334	338	327	304
13	294	294	288	284	282	280	s	266	s	s	253

s denotes a prominent shoulder or inflexion.

tra appear to conform with trends in the forsterite-fayalite and fayalite-tephroite series, as most bands (in the forsterite-tephroite series) move to lower frequencies with increasing manganese content.

Table 3. Peak maxima in the infrared spectra of manganiferous olivines.

Specimen No.	11	12	13	14	15	16	17	1 ^a	18	19	20
Band 1	945	944	945	944	944	965	973	985.4	958	970	975
2	914	913	912	912	909	924	933	957.3	918	948	931
3	872	872	870	868	860	871	872	886.9	871	879	900
4	827	825	823	821	818	822	827	839.3	824	829	869
5	558	560	565	562	564	580	588	611.0	572	595	613
6	506	504	505	504	505	504	507		508	513	577
7	472	475	477	478	481	s	485	508.7	480	475	459
8						412	440		410	438	394
9	356	355	357	352	348	362	374	420.6	358		379
12	304	311	305	297	290	319	335		307	303	217
13	253	250	250	241	240		265				

^a Extrapolated to 100% Mg₂SiO₄ using linear equations in table 4

s denotes a prominent shoulder or inflexion

In specimen 16, an additional peak occurs at 294 cm⁻¹

In specimen 17, an additional peak occurs at 415 cm⁻¹

In willemite (specimen 20), bands 10 and 11 occur at 266 and 227 cm⁻¹

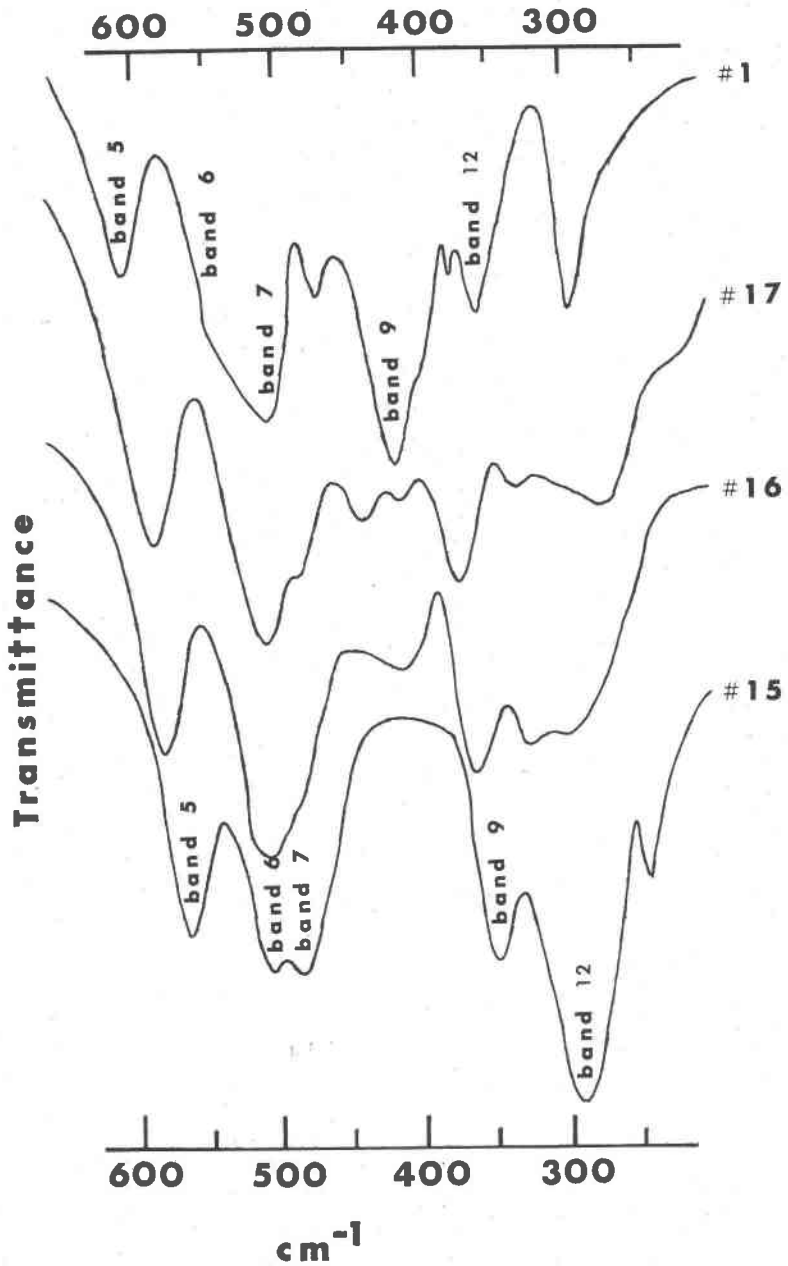


Fig. 5. Infrared spectra of Mg-Mn olivines of the forsterite-tephroite series.

The infrared spectrum of the zincian olivine roepperite (specimen 18) is comparable to those of Fe-Mn olivines and bears no resemblances to the spectrum of willemite containing tetrahedral Zn^{2+} (Figure 2). However, the band maxima for roepperite (specimen 18) summarized in Table 3 are displaced to lower frequencies than those for an Fe-Mn olivine (specimen 13) of similar Fe/Mn ratio.

DETERMINATIVE CURVES FROM THE INFRARED SPECTRA

Forsterite-Fayalite Series

The infrared spectra clearly demonstrate compositional variations of peak maxima in each of the binary olivine series, indicating that they form the basis of cation composition determinative curves. Best fitting polynomials were computed by the CURFIT program for eight bands in the infrared spectra of ten Mg-Fe olivines. The polynomials of best fit for all bands in this series were found to be linear equations, and are summarized in Table 4. These data relate the Mg_2SiO_4 component in an olivine (X) to peak maxima in the infrared spectra (ν). The sum of the squares of residuals, $\Sigma(|\nu_{obs} - \nu_{calc}|^2)$, are also given together with the standard deviations $d(n, q)$ in parentheses below each coefficient $c(n, q)$.

Table 4. Best-fit polynomials relating i.r. peak maxima to olivine composition in the forsterite-fayalite series.

Band in i.r. spectrum	Equation of best-fitting polynomial ($X = \% Mg_2SiO_4$)	Residual $\Sigma(\nu_{obs} - \nu_{calc} ^2)$
1	$\nu = 943.79 + 0.439X$ (1.48) (0.24)	38.35
2	$\nu = 912.71 + 0.433X$ (1.35) (0.22)	31.89
3	$\nu = 872.83 + 0.144X$ (0.55) (0.09)	5.34
4	$\nu = 826.78 + 0.124X$ (0.26) (0.04)	1.19
5	$\nu = 557.13 + 0.517X$ (0.58) (0.10)	5.84
7	$\nu = 471.54 + 0.346X$ (1.38) (0.23)	33.26
9	$\nu = 356.01 + 0.646X$ (1.17) (0.19)	23.97
(1+2+3+4 +5+7+9)	$\nu = 4942.80 + 2.646X$ (3.66) (0.59)	86.21
(4-5)	$\nu = 269.64 - 0.393X$ (0.94) (0.15)	5.74

Any of the equations in Table 4 could be used as an olivine cation composition determinative curve. However, certain bands are preferable to others. Bands 4 and 5 are considered to be the most suitable ones for determinative curves in the forsterite-fayalite series (Burns and Huggins, 1970) because they are sharp, relatively free from overlap with neighboring bands, and also show an adequate frequency range between end member compositions.

Other determinative curves may be computed from the peak maxima data summarized in Table 2. For example, the sum of the seven bands included in Table 4 has a large range (200 cm^{-1}) but has a large cumulative error arising from any error in spectra alignment. Calibration errors are reduced in determinative curves derived from the difference of bands 4 and 5, for example. Such difference polynomials eliminate alignment errors and problems of standardization between different infrared spectrometers. For example, we also computed best-fit polynomials for bands 4, 5, and (4-5) from the data of Lyon (1962) and Duke and Stephens (1964). When compared with the polynomials in Table 4, significant differences are found between the three sets of linear equations for bands 4 and 5, but there is good agreement between the sets of coefficients for band (4-5).

Fayalite-Tephroite Series

A selection of polynomials computed from the infrared spectra of Fe-Mn olivines is presented in Table 5. They give the Mn_2SiO_4 component in the olivine (X) as a function of peak maxima (ν). The peak maxima show zero, small positive, or small negative compositional variations. Because of the small compositional variations, determinative curves for this series based on individual bands have limited accuracy. A more accurate determinative curve is represented by the equation for the difference band (4-7) since the gradient of band 4 is positive and is negative for band 7. This equation is also free of spectrometer alignment errors.

Forsterite-Tephroite Series

Only four analysed specimens were available for the Mg-Mn olivine series. One of these specimens contained about 7 percent Fe_2SiO_4 and peak maxima for the end-member Mg_2SiO_4 component were obtained by extrapolating the linear equations in Table 4 to zero Fe_2SiO_4 . Because of the limited number of samples, only polynomials up to degree two are included in Table 5 as expressions relating Mg_2SiO_4 component (X) to peak maxima (ν). On the basis of standard deviation and residual data, the most suitable equation for Mg-Mn

Table 5. Best-fit polynomials relating i.r. peak maxima to olivine composition for manganese olivines.

Band in i.r. spectrum	Equation of Best- fitting polynomial	Residual $\Sigma(v_{\text{obs}} - v_{\text{calc}} ^2)$
Fayalite - Tephroite Series (X mole % Mn_2SiO_4)		
1	$v = 944.40$ (0.24)	1.20
2	$v = 909.49 + 0.049X$ (0.55) (0.009)	1.32
3	$v = 859.45 + 0.308X - 0.0018X^2$ (0.62) (0.028) (0.003)	0.69
4	$v = 817.88 + 0.096X$ (0.13) (0.002)	0.07
5	$v = 564.88 - 0.060X$ (1.78) (0.029)	13.65
6	$v = 504.80$ (0.37)	2.80
7	$v = 481.30 - 0.092X$ (0.41) (0.007)	0.73
9	$v = 348.49 + 0.084X$ (0.80) (0.013)	1.72
(4-7)	$v = 336.58 + 0.188X$ (0.34) (0.006)	0.50
Forsterite - Tephroite Series (X mole % Mg_2SiO_4)		
1	$v = 943.00 + 0.921X - 0.0050X^2$ (3.00) (0.154) (0.0014)	8.31
2	$v = 908.19 + 0.624X - 0.0013X^2$ (1.57) (0.081) (0.0007)	2.28
3	$v = 861.35 + 0.285X$ (2.15) (0.038)	15.36
4	$v = 817.07 + 0.220X$ (0.42) (0.007)	0.58
5	$v = 563.34 + 0.645X - 0.0017X^2$ (2.28) (0.117) (0.0011)	4.82
9	$v = 347.38 + 0.489X + 0.0024X^2$ (1.34) (0.069) (0.0006)	1.66
(2-4)	$v = 90.70 + 0.434X - 0.0016X^2$ (2.06) (0.106) (0.0010)	3.93

olivine determinative curves are considered to be those for band 4 and the difference band (2-4).

Determinative Grid for Mg-Fe-Mn Olivines

Since Mg^{2+} , Fe^{2+} , and Mn^{2+} are the three principal cations in most

olivine minerals, it is theoretically possible to estimate the relative proportions of these cations from the positions of any two bands in an infrared spectrum. This suggests that a triangular diagram may be constructed from the infrared data to form a cation composition determinative grid for Mg-Fe-Mn olivines.

Figure 6 shows the determinative grid constructed from bands 4 and 5 in the infrared spectra. The choice of band 5 as the second band was based on the manner in which the band 4 and band 5 contours cross. Band 1 could also be used in place of band 5, but the accuracy of estimating the peak maxima of band 1 is considerably lower. The contours have been drawn as straight lines in Figure 6. Although this is true for band 4 in all three binary series, it is not strictly correct for band 5 since in the forsterite-tephroite series the best-fitting polynomial of this band is a quadratic equation.

DISCUSSION

Assessment of the Infrared Olivine Composition Determinative Curves

Analyses of four of the Mg-Fe olivines were not available initially. Their compositions were estimated by the linear equations given in

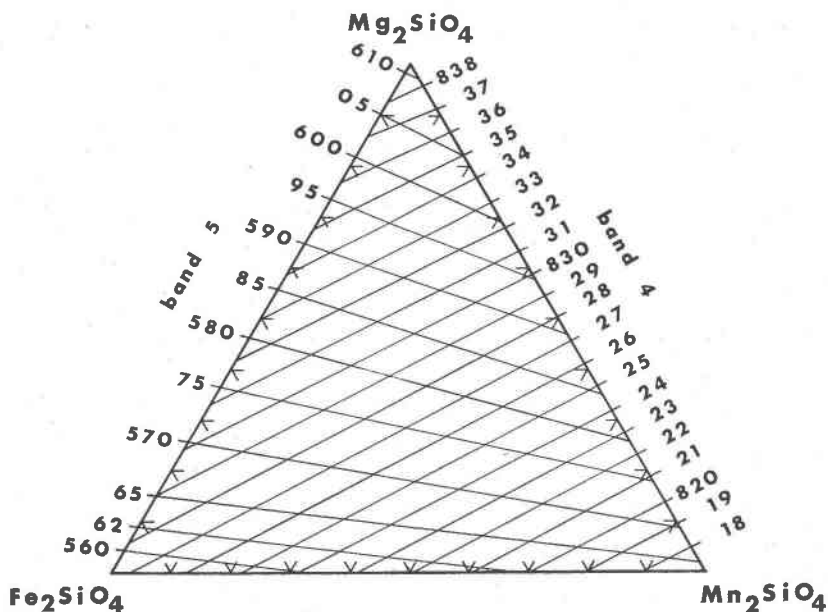


FIG. 6. Composition determinative grid for Mg-Fe-Mn olivines.

Table 4 and also by the determinative methods of Yoder and Sahama (1957) and Louisnathan and Smith (1968) based on X-ray data. The Mg_2SiO_4 components of the unanalysed olivines estimated by each of these determinative methods are summarized in Table 6, together with values ultimately obtained from microprobe analyses.

The data in Table 6 show that olivine compositions in the forsterite-fayalite series estimated from the infrared determinative curves are as close to the true compositions, if not closer, as the estimates based on the d_{130} spacings and cell parameter data.

The accuracy of an infrared determinative curve may be assessed as follows. An error $\delta\nu$ in peak position will cause an error δX in the determined mole percent X in the olivine. In the general case:

$$\nu \pm \delta\nu = c(n, 0) + c(n, 1)(X \pm \delta X) + \dots + c(n, n)(X \pm \delta X)^n$$

and

$$\nu = c(n, 0) + c(n, 1)X + \dots + c(n, n)X^n$$

Subtracting and ignoring second order terms and higher in X gives:

$$\pm \delta\nu = \pm \delta X [c(n, 1) + \dots + nc(n, n)X^{n-1}]$$

$$\delta\nu = \delta X \left(\frac{d\nu}{dX} \right)$$

or

$$\delta X = \delta\nu / \left(\frac{d\nu}{dX} \right)$$

Assuming an error of $\pm \epsilon \text{ cm}^{-1}$ arising from spectrometer alignment and personal reading errors, the error in composition estimated from a linear equation becomes

Table 6. Compositions of Selected Olivines estimated from Determinative Curves (% Mg_2SiO_4)

Specimen Number	Microprobe	Y&S ¹	L&S ²			Infrared Bands		
			a	b	c	4	5	4-5
3	78.9	79	74	75	72	77	74	78
4	59.3	70	65	62	66	61	58	62
5	60.0	61	69	59	59	61	66	60
10	20.2	--	--	--	--	22	18	24

¹ Yoder and Sahama (1957)

² Louisnathan and Smith (1968)

$$\delta X = \pm \epsilon / c(1, 1)$$

while for quadratic equations it is

$$\delta X = \pm \epsilon / [c(2, 1) + 2c(2, 2)X]$$

This analysis shows that for bands 4, 5, and (4-5) (the estimated peak positions of which are in error by a maximum of $\pm 1 \text{ cm}^{-1}$), the errors in the Mg_2SiO_4 components in Table 6 estimated from infrared spectroscopy are about ± 8 , ± 2 , and ± 3 percent, respectively (using the $c(1, 1)$ coefficients in Table 4).

While it was not possible to compare results based on infrared determinative curves for Fe-Mn olivines, the smaller compositional variations of peak maxima in the fayalite-tephroite series (and hence, the smaller $c(1, 1)$ coefficients) lead to larger errors in composition estimates. Thus, errors of 10, 10, and 5 percent are expected for bands 4, 7, and (4-7). Although $c(1, 1)$ and $c(2, 1)$ parameters are generally large for the linear and quadratic equations for the forsterite-tephroite series, the accuracy of the infrared composition determinative curves for Mg-Mn olivines is probably reduced because they are based on few available specimens.

The usefulness of the olivine composition determinative grid may be illustrated by the results obtained for specimen 8, which is a Mg-Fe olivine with appreciable manganese content (Table 1). The maxima of bands 4 and 5, 830 and 573 cm^{-1} respectively, for this specimen (Table 2) are located on the determinative grid in Figure 6 at the composition $(\text{Mg}_{0.31}\text{Fe}_{0.61}\text{Mn}_{0.08})_2\text{SiO}_4$. This composition is in good agreement with the formula derived from the electron microprobe analysis, $(\text{Mg}_{0.313}\text{Fe}_{0.624}\text{Mn}_{0.063})_2\text{SiO}_4$.

Evidence Bearing on Cation Ordering in Olivine

A significant feature of the infrared data is the nonlinear best-fit equations computed for many of the determinative curves of manganese olivines, which contrasts with the linearity of all best-fit equations for Mg-Fe olivines. Since Mn^{2+} ions are enriched in the olivine $M(2)$ positions (Burns, 1970), this suggests that peak-maxima—olivines composition data are not linear whenever appreciable cation ordering occurs in the olivine structure.

Such non-linearity implies that the vibrational frequencies are site dependent. If the vibrations were equally influenced by cations in the $M(1)$ and $M(2)$ positions, then the determinative curves for manganese olivines would be linear and reflect only the bulk chemical

composition of the olivine. Equations which are non-linear all have negative $c(2, 2)$ coefficients (Table 5). If linear equations derived from end-member spectra were used as determinative curves, the estimated Mn content of intermediate olivines would be lower than the real values based on quadratic equations. This indicates that the vibrations are influenced more by Mg^{2+} and Fe^{2+} ions in manganese olivines, which are known (Burns, 1970) to be enriched in the $M(1)$ sites. Further corroborative evidence of $M(1)$ site occupancy affecting vibrational frequencies stems from the spectra of synthetic $\gamma-Ca_2SiO_4$, $CaMgSiO_4$, and Mg_2SiO_4 (Tarte, 1963). Again the positive deviation in the infrared data of intermediate $CaMgSiO_4$ correlates with the ordering of Mg^{2+} ions in the $M(1)$ positions of monticellite.

The linearity of the peak-maxima—olivine composition data for the Mg-Fe olivine series indicates that the occupancy of the $M(1)$ positions not only reflects the bulk composition of the olivine but also indicates a nearly random distribution of Mg^{2+} and Fe^{2+} ions over the $M(1)$ and $M(2)$ positions in the olivines used in the present study. Conversely, any significant deviation of the infrared data of a given analysed Mg-Fe olivine from the linear determinative curves presented in Table 4 implies ordering of Mg^{2+} and Fe^{2+} ions.

ACKNOWLEDGMENTS

We wish to thank sincerely several mineralogists who made available specimens for this study. These include: Dr. S. O. Agrell, Dr. F. B. Atkins, Dr. G. E. Brown, Professor J. C. Carpenter, Dr. P. G. Embrey, Professor G. V. Gibbs, Professor C. S. Hurlbut Jr., Dr. B. Mason, Professor A. Pabst, and Professor E. A. Vincent. Microprobe analyses were performed by Dr. R. K. O'Nions and Professor D. G. W. Smith (Calgary), and Dr. D. C. Harris (Ottawa). Information in advance of publication was received from Dr. G. E. Brown and Professor G. V. Gibbs. Penny Sharp and Sue Hall assisted in the preparation and editing of the manuscript. Financial assistance from NASA Grant No. NGR-22-009-551 is acknowledged.

REFERENCES

- AGTERBERG, F. P. (1964) Statistical analysis of X-ray data for olivine. *Mineral. Mag.* 33, 742-748.
- BANCROFT, G. M., AND R. G. BURNS (1969) Mossbauer and absorption spectral study of amphiboles of the glaucophane—riebeckite series. *Mineral. Soc. Amer. Spec. Pap.* 2, 137-148.
- BLOSS, F. D. (1952) Relationship between density and composition in mol. percent for some solid solution series. *Amer. Mineral.* 37, 966-981.
- BOWEN, N. L., AND J. SCHAIRER (1935) The system $MgO-FeO-SiO_2$. *Amer. J. Sci.* 29, 151-217.
- BURNS, R. G. (1970) Crystal field spectra and evidence of cation ordering in olivine minerals. *Amer. Mineral.* 55, 1608-1632.

- , AND F. E. HUGGINS (1970) Cation determinative curves and evidence of ordering in Mg-Fe-Mn olivines from vibrational spectra. *Geol. Soc. Amer. Ann. Meet. Abstr.*, 511-512.
- , AND F. J. PRENTICE (1968) Distribution of iron cations in the crocidolite structure. *Amer. Mineral.* 53, 770-776.
- DEER, W. A., R. A. HOWIE, AND J. ZUSSMAN (1963) *Rock-Forming Minerals*. Longmans, Green and Co., Ltd., London.
- DUKE, D. A., AND J. D. STEPHENS (1964) Infrared investigation of the olivine group minerals. *Amer. Mineral.* 49, 1388-1406.
- ELISEEV, E. N. (1957) X-ray study of the minerals of the isomorphous series forsterite-fayalite. *Zap. Vses. Mineral. Obshch. Ser. 2*, 86, 657-670.
- FISHER, G. W., AND L. G. MEDARIS (1969) Cell dimensions and X-ray determinative curve for synthetic Mg-Fe olivines. *Amer. Mineral.* 54, 741-753.
- GLASSER, F. P., AND E. F. OSBORN (1960) The ternary system MgO-MnO-SiO₂. *J. Amer. Ceram. Soc.* 43, 132-140.
- HECKROODT, R. O. (1958) An X-ray method for the determination of olivine. *Trans. Geol. Soc. S. Afr.* 61, 377-386.
- HENRIQUES, A. (1968) The effect of cations on the optical properties and cell dimensions of knebelite and olivine. *Arkiv. Mineral. Geol.* 2, 305.
- HOTZ, P. E., AND E. D. JACKSON (1963) X-ray determinative curve for olivines of composition Fo₉₀₋₉₅ from stratiform and alpine type peridotites. *U. S. Geol. Surv. Prof. Pap.* 450E, 101-102.
- HURLBUT, JR., C. S. (1961) Tephroite from Franklin, New Jersey. *Amer. Mineral.* 46, 549-559.
- JACKSON, E. D. (1960) X-ray determinative curve for natural olivine composition Fo₉₀₋₉₅. *U. S. Geol. Surv. Prof. Pap.* 400B, 432-434.
- JAHANBAGLOO, I. C. (1969) X-ray diffraction study of olivine solid solution series. *Amer. Mineral.* 54, 246-250.
- JAMBOR, J. L., AND C. H. SMITH, (1968) Olivine composition determinative curve with small diameter X-ray camera. *Mineral. Mag.* 33, 730-741.
- LEHMANN, H., H. DUTZ, AND M. KOLTERMANN (1961) Ultrarotspektroskopische Untersuchungen zur Mischkristallreihe Forsterit-Fayalit. *Ber. Deut. Keram. Ges.* 38, 512-514.
- LOUISNATHAN, S. J., AND J. V. SMITH (1968) Cell dimensions of olivine. *Mineral. Mag.* 36, 1123-1134.
- MASON, B. (1959) Tephroite from Clark Peninsula, Wilkes Land, Antarctica. *Amer. Mineral.* 44, 428-430.
- MATSUI, Y., AND Y. SYONO (1968) Unit cell dimensions of some synthetic olivine group solid solutions. *Geochem. J.* 2, 51-59.
- MOEHLMAN, R. S., AND F. A. GONYER (1934) Monticellite from Crestmore, California. *Amer. Mineral.* 19, 474-476.
- NAFZIGER, R. H., AND A. MUAN (1967) Equilibrium phase compositions and thermodynamic properties of olivines and pyroxenes in the MgO-FeO-SiO₂ system. *Amer. Mineral.* 52, 1364-1385.
- POLDERVAART, A. (1950) Correlation of physical properties and chemical composition in the plagioclase, olivine and orthopyroxene series. *Amer. Mineral.* 35, 1067-1079.
- SAHAMA, T. G., AND D. R. TORGESON (1949) Thermochemical studies of the olivines and orthopyroxenes. *U. S. Bur. Mines Rep. Invest.* 4408, 24 pp.

- SMITH, J. V. (1966) X-ray emission microanalysis of rock-forming minerals. II Olivines. *J. Geol.* **4**, 1-16.
- TARTE, P. (1963) Etude infra-rouge des orthosilicates et des orthogermanates. II. Structures du type olivine et monticellite. *Spectrochim. Acta*, **19**, 25-47.
- YODER, H. S., AND T. G. SAHAMA (1957) Olivine X-ray determinative curve. *Amer. Mineral.* **42**, 475-491.

Manuscript received, June 30, 1971; accepted for publication, December 27, 1971.